

Stone Soup: ADS-B-based Multi-Target Tracking with Stochastic Integration Filter

John Hiles*, Jakub Matoušek[†], Erik Blasch[‡], Ruixin Niu*, Ondřej Straka[†], Jindřich Duník[†]

*Dept. of ECE, Virginia Commonwealth Univ., Richmond, VA, USA

{hilesj, rniu}@vcu.edu

[†]Dept. of Cybernetics, Univ. of West Bohemia, Pilsen, Czech Republic

{matoujak, straka30, dunikj}@kky.zcu.cz

[‡]MOVEJ Analytics, Fairborn, OH, USA

erik.blasch@gmail.com

Abstract—This paper focuses on the multi-target tracking using the Stone Soup framework. In particular, we aim at evaluation of two multi-target tracking scenarios based on the simulated class-B dataset and ADS-B class-A dataset provided by OpenSky Network. The scenarios are evaluated w.r.t. selection of a local state estimator using a range of the Stone Soup metrics. Source code with scenario definitions and Stone Soup set-up are provided along with the paper.

Index Terms—multi-target tracking, state estimation, stochastic integration rule, Stone Soup, ADS-B.

I. INTRODUCTION

In the past few decades, there has been a lot of interest in nonlinear state estimation of stochastic dynamic systems using noisy observations. Nonlinear state estimators can be largely divided into two categories: global and local filters. Global filters, such as the ensemble Kalman filter (EnKF) [13], point-mass filter [9], and particle filter [25], provide the approximated posterior probability density function (PDF) of the system state. On the other hand, to take advantage of the Kalman filter’s recursive framework and achieve lower computational complexity, local filters, such as the extended Kalman filter (EKF) [3], unscented Kalman filter (UKF) [16], cubature Kalman filter (CKF) [2], and Monte Carlo Kalman filter (MCKF) [30], calculate the conditional mean and covariance matrix instead of the posterior PDF.

In comparison to other local filters, the *stochastic integration filter* (SIF) [10], offers an asymptotically accurate integral evaluation of the conditional mean and covariance matrix, with reasonable computation complexity. When selecting some of the SIF’s random parameters deterministically, the UKF and CKF are special cases of the SIF. The SIF has been shown to provide improved tradeoff between estimation accuracy and computational complexity, in comparison to the EnKF, MCKF, EKF, and UKF [8], [11]. In [8], the SIF was implemented in Python and incorporated in the Stone Soup framework. However, the testing scenarios in [8] only involve a single target and simulated data. The focus of this

paper is to investigate the performance of the SIF for multi-target tracking (MTT) using both simulated and real automatic dependent surveillance–broadcast (ADS-B) data in the Stone Soup framework.

A. Multitarget Tracking in ABS-B

MTT has widely been explored since the 1960’s to support surveillance, navigation, and control. Popular MTT algorithms include the joint probabilistic data association filter (JPDAF) [3], multiple hypothesis tracking (MHT) [5], random finite set (RFS) based filters [17], [18], [32], and message passing based algorithms [19]. Typically, MTT includes measurement pre-processing, estimation, and prediction to monitor a coverage area. Measurement pre-processing is usually applied to increase the signal-to-noise ratio (SNR). Estimation includes the refinement of the state to reduce the error and prediction uses the current state estimate to predict the future expected measurement location. Among the MTT steps, resolving the measurement to the correct target is data association which is a key challenge. Hence, the associations within MTT include measurement-to-measurement association, measurement-to-track association, and track-to-track association. To research these needs among filtering techniques, scenarios, and metrics, the ISIF community has developed the open source Stone Soup collection. Managed by the ISIF Open Source Tracking and Estimation Working Group (OSTEWG) [22], an emerging set of scenarios and metrics afford the comparison of contemporary methods – such as the SIF.

For this paper, the scenario of choice was to research the ADS-B scenario based on the OpenSky data. ADS-B data has grown in popularity for research since its mandated use for aerospace systems in the early 2010s for full scale operation in 2020. Currently, the data is accessible from FightRadar24 to track all the aircraft in the sky that are reporting. Hence, with the ADS-B, methods for air traffic management (ATM) can be assessed to improve efficiency, safety, and reliability for increasing the density of airspace that includes military (e.g., surveillance), commercial (e.g., passengers), and business operations (e.g., air package delivery). At the same time, since the ADS-B is air traffic, similar constructs for ground

O. Straka and J. Duník have been in part supported by the Ministry of Education, Youth and Sports of the Czech Republic under project ROBOPROX - Robotics and Advanced Industrial Production CZ.02.01.01/00/22_008/0004590.

(transponders) and maritime (automatic identification system AIS) are being considering for space operations for space traffic management (STM). With such a capability, research is emerging on the efficacy of the methods in response to measurement attacks of spoofing, jamming, and replay.

B. Goal of the Paper

In this paper, we simulate two scenarios using the Stone Soup framework;

- (i) Simulation involving several overlapping trajectories. In this scenario, the bearing, range, and elevation measurements are sequential and without clutter.
- (ii) Usage of the OpenSky aircraft ADS-B data as ground truth and simulation of the bearing, range, elevation detections from multiple sensors introducing the clutter.

These two MTT scenarios are implemented using the EKF, UKF, and the SIF selected as the state estimators. The MTT performance is evaluated using multiple metrics including the optimal sub-pattern assignment and single integrated air picture position accuracy. The source codes are provided along with the paper¹.

The rest of the paper is organized as follows. In Section II the Stone Soup framework is reviewed. Section III focuses on brief introduction of the MTT with an emphasis on the local filter design. Then, Section IV describes considered blocks of Stone Soup used in the numerical experiments. The experiments are discussed in Sections V and VI for class-B aerospace and ADS-B datasets, respectively. The concluding remarks are drawn in Section VII.

II. STONE SOUP

The Stone Soup project project is an open-source tracking and estimation framework currently available as a python library; to support developers, users, and systems engineers. The framework saw its first public alpha release in 2017 [31] with the first beta release in 2019. The name of the framework is inspired by the tale of the “Stone Soup”; from European folklore in which many ingredients (estimation methods) are contributed by villagers (researchers) to devise a flavourful soup(useful software). Inherent in the common repository is the ability to compare and reuse contributions to extend the quality of the estimation capabilities. While some have sought initial ideas [6], [14], Barr et al. [4] highlight the many capabilities such as track generation, filtering, classification, data association, and sensor management routines. Since then the Stone Soup has been extended with a variety of components and routines [7], [8], [36] and offers the following tools for end-to-end solution of the MTT task:

- 1) **Track generator** - For comparative analysis, the truth generator enables track initiation, trajectory analysis, and modifications such as emulating an outage.
- 2) **Track association** - A simulator provides control over the data association between measurements and targets.

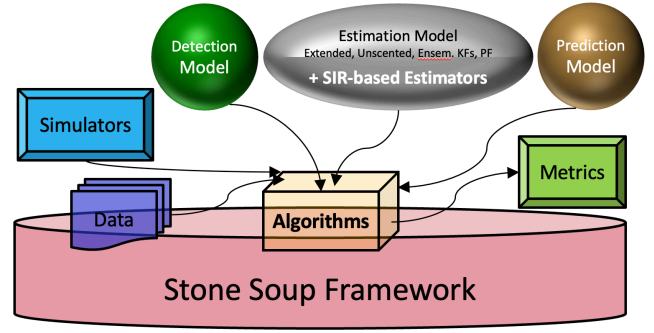


Fig. 1. Elements of the ISIF Stone Soup framework [8].

- 3) **Track metrics** - The Stone Soup repository offers a variety of contemporary measures, including:

- Weighted Euclidean distance measure,
- Squared Mahalanobis distance measure,
- Squared Gaussian Hellinger distance measure,
- Kullback–Leibler divergence,
- Generalized Optimal Subpattern Assignment.

The Standardized Information and Analysis Program measures includes:

- Ambiguity,
- Completeness,
- Longest tracking,
- Track rate spuriousness,
- Velocity and position accuracy.

- 4) **Track estimators** - Considering measurement-to-track association, the target state can be estimated by a number of filters offering a trade-off between complexity and accuracy, such as:

- EKF, UKF, SIF,
- Particle filters.

Additional features include track deletion, handling out-of-order sequences, and density management.

The overall scheme of the Stone Soup framework with the SIR-based estimators is illustrated in Fig. 1.

III. MULTIPLE TARGET TRACKING AND STATE ESTIMATION

Multitarget tracking is a well-developed and wide area that aims at estimation of the state an unknown number $n_k \geq 0$ of targets based on the a number $m_k \geq 0$ of measurements at time-step k . Whereas the state includes for example, position and velocity, of each tracked target (or object) and is unknown, the measurement can be seen as an available noisy nonlinear transformation of the state, for example in the form of range and bearing of each target w.r.t. a radar. As the measurements are imperfect and cluttered, the number of tracked targets n_k and available measurements m_k need not be equal and has to be associated. This measurement to target state association can be addressed by a variety of methods including the well-known and in the Stone Soup implemented JPDAF and MHT algorithms [4].

¹<https://github.com/0sm1um/ADS-B-Tracking>

Having the association performed, that the state of each target is estimated by a dedicated, in our case local, filter. In this paper, we focus on the assessment of the local filter selection on the performance of the whole MTT system. Therefore, in the following parts, we briefly introduce the state-space model for the target modeling and the local state estimator design for the its state estimation.

A. State-Space Model

The target motion can be conveniently described by a discrete-time stochastic dynamic state-space model with linear dynamics and nonlinear measurement equation

$$\mathbf{x}_{k+1} = \mathbf{F}_k \mathbf{x}_k + \mathbf{w}_k, \quad (1)$$

$$\mathbf{z}_k = \mathbf{h}_k(\mathbf{x}_k) + \mathbf{v}_k, \quad (2)$$

where the vectors $\mathbf{x}_k \in \mathbb{R}^{n_x}$ and $\mathbf{z}_k \in \mathbb{R}^{n_z}$ represent the *unknown and sought* state of the system and the *available* measurement at time instant k , respectively, and $k = 0, 1, 2, \dots, T$. The state transition matrix $\mathbf{F}_k : \mathbb{R}^{n_x \times n_x}$ and the measurement function $\mathbf{h}_k : \mathbb{R}^{n_x} \rightarrow \mathbb{R}^{n_z}$ are supposed to be known. The state dynamics can be described by a number of models including nearly constant velocity, known/unknown turn-rate, or a Singer models, to name a few. The measurement equation depends on the sensors employed. If a radar is used, then the measurement consists of the range and bearing angle between the target and the radar.

The state noise $\mathbf{w}_k \in \mathbb{R}^{n_x}$, the measurement noise $\mathbf{v}_k \in \mathbb{R}^{n_z}$, and the initial state $\mathbf{x}_0 \in \mathbb{R}^{n_x}$ are supposed to be independent of each other. The noises and the initial state are assumed to be normally distributed, i.e.,

$$p(\mathbf{w}_k) = \mathcal{N}\{\mathbf{w}_k; \mathbf{0}_{n_x \times 1}, \mathbf{Q}_k\}, \quad (3)$$

$$p(\mathbf{v}_k) = \mathcal{N}\{\mathbf{v}_k; \mathbf{0}_{n_z \times 1}, \mathbf{R}_k\}, \quad (4)$$

$$p(\mathbf{x}_0) = \mathcal{N}\{\mathbf{x}_0; \bar{\mathbf{x}}_0, \mathbf{P}_0\}, \quad (5)$$

where $\mathbf{0}_{n_x \times 1} \in \mathbb{R}^{n_x \times 1}$ is a zero vector and the notation $\mathcal{N}\{\mathbf{x}; \bar{\mathbf{x}}, \mathbf{P}\}$ stands for the Gaussian PDF of a random variable \mathbf{x} with mean $\bar{\mathbf{x}}$ and covariance matrix \mathbf{P} . The first two moments of the random variables in (3)–(5) are supposed to be known.

B. Extended, Unscented, Cubature, and Stochastic Integration Filters

The EKF, UKF, CKF, and SIF are representatives of the *local approaches* to state estimation [27], [34]. In particular, the local filters provide the estimate of the state \mathbf{x}_k conditioned on all available measurements $\mathbf{z}^k = [\mathbf{z}_0, \mathbf{z}_1, \dots, \mathbf{z}_k]$ and the state-space model (1)–(5) in the form of the filtering conditional mean and covariance matrix defined as

$$\hat{\mathbf{x}}_{k|k} = \mathbb{E}[\mathbf{x}_k | \mathbf{z}^k], \quad (6)$$

$$\hat{\mathbf{P}}_{k|k}^{xx} = \text{cov}[\mathbf{x}_k | \mathbf{z}^k]. \quad (7)$$

In the Bayesian framework, the mean and the covariance matrix can be interpreted as a moments defining the *approximate Gaussian* filtering PDF

$$p(\mathbf{x}_k | \mathbf{z}^k) \approx \mathcal{N}\{\mathbf{x}_k; \hat{\mathbf{x}}_{k|k}, \hat{\mathbf{P}}_{k|k}^{xx}\}. \quad (8)$$

Respecting the Bayesian perspective for local filter design, the algorithm of any local filter reads:

Algorithm: Generic Local Filter

Step 1: Set the time instant $k = 0$ and define an initial condition $p(\mathbf{x}_0 | \mathbf{z}^0) = \mathcal{N}\{\mathbf{x}_0; \hat{\mathbf{x}}_{0|-1}, \mathbf{P}_{0|-1}^{xx}\}$.

Step 2: The moments of the filtering estimate $p(\mathbf{x}_k | \mathbf{z}^k) \approx \mathcal{N}\{\mathbf{x}_k; \hat{\mathbf{x}}_{k|k}, \mathbf{P}_{k|k}^{xx}\}$ are

$$\hat{\mathbf{x}}_{k|k} = \hat{\mathbf{x}}_{k|k-1} + \mathbf{K}_k(\mathbf{z}_k - \hat{\mathbf{z}}_{k|k-1}), \quad (9)$$

$$\mathbf{P}_{k|k}^{xx} = \mathbf{P}_{k|k-1}^{xx} - \mathbf{K}_k \mathbf{P}_{k|k-1}^{zz} \mathbf{K}_k^T, \quad (10)$$

where $\mathbf{K}_k = \mathbf{P}_{k|k-1}^{xz} (\mathbf{P}_{k|k-1}^{zz})^{-1}$ is the filter gain,

$$\hat{\mathbf{z}}_{k|k-1} = \int \mathbf{h}_k(\mathbf{x}_k) \mathcal{N}\{\mathbf{x}_k; \hat{\mathbf{x}}_{k|k-1}, \mathbf{P}_{k|k-1}^{xx}\} d\mathbf{x}_k, \quad (11)$$

$$\begin{aligned} \mathbf{P}_{k|k-1}^{zz} &= \int (\mathbf{h}_k(\mathbf{x}_k) - \hat{\mathbf{z}}_{k|k-1})(\cdot)^T \\ &\times \mathcal{N}\{\mathbf{x}_k; \hat{\mathbf{x}}_{k|k-1}, \mathbf{P}_{k|k-1}^{xx}\} d\mathbf{x}_k + \mathbf{R}_k, \end{aligned} \quad (12)$$

$$\begin{aligned} \mathbf{P}_{k|k-1}^{xz} &= \int (\mathbf{x}_k - \hat{\mathbf{x}}_{k|k-1})(\mathbf{h}_k(\mathbf{x}_k) - \hat{\mathbf{z}}_{k|k-1})^T \\ &\times \mathcal{N}\{\mathbf{x}_k; \hat{\mathbf{x}}_{k|k-1}, \mathbf{P}_{k|k-1}^{xx}\} d\mathbf{x}_k. \end{aligned} \quad (13)$$

Step 3: The predictive moments of the Gaussian-assumed PDF $p(\mathbf{x}_{k+1} | \mathbf{z}^k) \approx \mathcal{N}\{\mathbf{x}_{k+1}; \hat{\mathbf{x}}_{k+1|k}, \mathbf{P}_{k+1|k}^{xx}\}$ are calculated according

$$\hat{\mathbf{x}}_{k+1|k} = \mathbb{E}[\mathbf{x}_{k+1} | \mathbf{z}^k] = \mathbf{F}_k \hat{\mathbf{x}}_{k|k}, \quad (14)$$

$$\mathbf{P}_{k+1|k}^{xx} = \mathbb{E}[\mathbf{x}_{k+1} | \mathbf{z}^k] = \mathbf{F}_k \mathbf{P}_{k|k}^{xx} \mathbf{F}_k^T + \mathbf{Q}_k. \quad (15)$$

The algorithm then continues to **Step 2** with $k \leftarrow k + 1$.

The evaluation of the expected values (11)–(13) for the measurement prediction in the filtering step can be seen as a calculation of the moments of a nonlinearly transformed Gaussian random variable with known description [21], [34]. This means that calculation of the moments can be interpreted as an evaluation of a *Gaussian-weighted* integral

$$\mathcal{I} = \mathbb{E}[\mathbf{g}(\mathbf{x}_k) | \mathbf{z}^{k-1}] = \int \mathbf{g}(\mathbf{x}_k) \mathcal{N}\{\mathbf{x}_k; \hat{\mathbf{x}}_{k|k-1}, \mathbf{P}_{k|k-1}^{xx}\} d\mathbf{x}_k, \quad (16)$$

where the conditional mean $\hat{\mathbf{x}}_{k|k-1}$ and the covariance matrix $\mathbf{P}_{k|k-1}^{xx}$ are known from estimator preceding steps and the nonlinear function $\mathbf{g}(\cdot)$ stems from the model and calculated moment definition (namely mean or covariance matrix evaluation).

Closed-form solution to the Gaussian weighted integrals is possible for a narrow class of functions $\mathbf{h}_k(\cdot)$, such as the *linear* function for which any local filter becomes the optimal Kalman filter. For nonlinear case, an approximate solution has to be used. In the area of the local filters two principal approximation can be used, namely (i) linearisation of nonlinear model functions allowing an *analytical* solution to (16), (ii) approximation of the weighting Gaussian PDF by a set weighted points enabling a *numerical* solution to (16).

The former approximation is based on the linearisation of the nonlinear functions by the Taylor expansion or the Stirling's interpolation, which leads e.g., to the EKF, second order filter, or the divided difference filters [1], [20], [27]. The latter approximation allows solution to the integral (16) by a quadrature or cubature numerical integration rule of the form

$$\mathcal{I} \approx \hat{\mathcal{I}} = \sum_{i=1}^S \omega^{(i)} \mathbf{g}(\boldsymbol{\xi}_{k|k-1}^{(i)}), \quad (17)$$

where $\boldsymbol{\xi}_{k|k-1}^{(i)}$ and $\omega^{(i)}$ are spherical-radial points and corresponding weights of the rule, respectively. This class of local filters is represented by the SIF, unscented or cubature Kalman filters [2], [11], [12], [15]. Although both approaches are based on different ideas and approximations, the resulting algorithms can be written in a unified form [34].

C. Expected Performance of Filters and the Goal of the Paper

The EKF is probably the most used algorithm in the tracking and navigation, and this is due to several reasons; it is (i) a widely known algorithm (for a couple of decades), (ii) computationally efficient and with a plethora of stable implementations [1], [29], and (iii) a certifiable algorithm for a civil aircraft navigation system [26]. On the other hand, the EKF performance may degrade for models with a higher degree of nonlinearity or higher uncertainty, where the linearisation is not valid anymore. In this case, the EKF may provide inconsistent (namely optimistic) estimates, i.e., estimate covariance matrix $\mathbf{P}_{k|k}$ does not correspond to the true mean estimate error $\tilde{\mathbf{x}}_{k|k} = \mathbf{x}_k - \hat{\mathbf{x}}_{k|k}$. Based on extensive analysis and numerical verification, the SIF seems to be a more robust algorithm (not only w.r.t. EKF, but also UKF and CKF) for models with a higher degree of nonlinearity providing a consistent estimate [8], [11], [37]. The reason can be found in a more realistic assessment of the estimate uncertainty. On the other hand, the SIF has higher computational complexity.

The *goal* of the paper is to assess the impact of the selected local filters on the performance of the MTT system which might be seen as a complex nonlinear problem. The assessment is performed using the Stone Soup framework with simulated and OpenSky Network downloaded data.

IV. STONE SOUP IMPLEMENTATION DESCRIPTION

Having the filters introduced, we briefly describe the overall setting of the multi-target tracking task in the Stone Soup framework. Description of the Stone Soup components used in our implementation and simulations, including the tracker architecture and the metrics employed for performance evaluation, follows.

A. Tracker

The implemented MTT system employs the global nearest neighbour (GNN) data association method with a 2D assignment algorithm. This setup ensures efficient and accurate association between predicted tracks and incoming detections. The classes used for the MTT tracker are:

- **Data Associator** (routine *GNNWith2DAssignment*): Utilizes the GNN to associate detections (or radar measurements) to predicted target states. This method constructs a 2D matrix of distances between predictions and detections and solves the assignment problem to find the optimal associations.
- **Distance Hypothesiser**: Generates assignment hypotheses based on the distance between predicted and detected states, using the Mahalanobis distance measure. *Parameters*:
 - Mahalanobis distance calculates the distance between predicted and detected states.
 - Missed detection distance threshold is set to 5. If the distance between a predicted state and a detection exceeds this value, the detection is considered a missed detection. This parameter helps in managing associations in cluttered environments by limiting the consideration of unlikely associations.
- **Target Deleter**: Deleter is a component used to remove targets from the tracking system based on the time since their last prediction or update. It is configured with a time threshold, and targets are deleted if they have not been updated or predicted within this threshold period. *Parameters*:
 - Time threshold is set to $t = 10$.

This configuration ensures robust tracking performance by effectively managing data association, even in the presence of clutter and missed detections. Although for the purpose of this paper, we are not considering clutter.

B. Filters

The MTT system is designed with two filters, namely the *standard* EKF and the *robust* third-order SIF [8]. Note that the UKF, when run with the default parameters in Stone Soup, experienced stability issues, resulting in a covariance matrix that was not semidefinite positive.

C. Metrics

To evaluate the performance of the MTT system in the presence of clutter, we employ the following standard metrics² from the Stone Soup framework:

- **Optimal Sub-Pattern Assignment (OSPA)**: The OSPA metric quantifies the accuracy of the estimated target states compared to the ground truth by considering both localization errors and cardinality errors. It provides a balanced assessment of multi-target tracking performance, penalizing both position estimation errors and missed or false detections. *Parameters*:
 - Norm associated to distance is p .
 - Maximum distance for possible association is c .

Parameter p can be generally thought of as the sensitivity to outliers [23] in tracks. $p = 2$ is used for both examples. Parameter c is associated with the degree to

²https://stonesoup.readthedocs.io/en/latest/auto_examples/metrics/Metrics.html

which Cardinality errors dominate the metric. Lower values of c tend to favor the precision of tracks, and higher values disregard locality errors. Optimal choice of c primarily depends on the magnitude of a typical locality error (distances between a track and a truth) and hence the Class-B Airspace example uses $c = 10$ and the Class-A Airspace example uses $c = 250$.

- **Single Integrated Air Picture (SIAP) Ambiguity** [33]: The SIAP ambiguity metric assesses the number of tracks assigned to a true object. A score of 1 is optimal.

$$A = \frac{\sum_{k=0}^T N_{A,k}}{\sum_{k=0}^T J_{T,k}}, \quad (18)$$

where $N_{A,k}$ represents the number of associated tracks at a given time, and $J_{T,k}$ represents the number of associated true targets.

- **Single Integrated Air Picture (SIAP) Position Accuracy** [33]: The SIAP position accuracy metric assesses the mean positional error of the estimated tracks relative to ground truth. The Positional Accuracy Metric is given as:

$$PA = \frac{\sum_{k=0}^T \sum_{n \in D_k} PA_{n,k}}{\sum_{k=0}^T N_{A,k}}, \quad (19)$$

where D_k is the set of tracks held at timestamp k and $PA_{n,k}$ is the Euclidean distance of track n to its associated truth at the corresponding timestamp.

- **Sum of Covariance Norms:** This metric evaluates the overall uncertainty in state estimation by summing the Frobenius norms of the estimated covariance matrices across all tracked targets. A lower value indicates more confident and precise state estimates, while a higher value suggests greater uncertainty in tracking results [24]. The Frobenius Norm used and corresponding metric are given as:

$$\|\mathbf{P}_{k|k}^{xx}\|_F = \sqrt{\text{tr}((\mathbf{P}_{k|k}^{xx})^T \mathbf{P}_{k|k}^{xx})}.$$

These metrics collectively provide a comprehensive evaluation of the tracking performance, balancing accuracy, robustness, and uncertainty quantification in a cluttered MTT environment.

V. SIMULATED CLASS-B AIRSPACE DATASET

Presented here is a scenario of crowded airspace, typically from the surface to 10,000 $[ft]$ above sea level. Class-B Airspace is a designation typically reserved for the busiest airports in a country. All aircraft operating in Class B Airspace typically need clearance from Air Traffic Controllers to fly, and Class-B Airspace is typically very closely monitored as it is the zone in which collisions are most probable.

A. Simulation Parameters

In this scenario, 10 maneuvering targets in a relatively enclosed 2D airspace are simulated. All targets start with randomly generated initial position within a 30 $[km]$ by

300 $[km^2]$. All targets have velocities in two dimensions randomly initialized between ± 200 $[m/s]$.

Each target state is defined as its position in $[m]$ and velocity in $[m/s]$ in north direction and in east direction, i.e., $\mathbf{x}_k = [p_{N,k}, v_{N,k}, p_{E,k}, v_{E,k}]^T = [\mathbf{x}_{1,k}, \mathbf{x}_{2,k}, \mathbf{x}_{3,k}, \mathbf{x}_{4,k}]^T$, $\mathbf{x}_{i,k}$ stands for i -th element of the vector \mathbf{x}_k . The state of each target can follow one of the following *three* motion models, namely

- Nearly constant velocity (NCV) model with matrices defining the state equation (1)

$$\mathbf{F}_k = \begin{bmatrix} 1 & dt & 0 & 0 \\ 0 & 1 & 0 & 0 \\ 0 & 0 & 1 & dt \\ 0 & 0 & 0 & 1 \end{bmatrix}, \mathbf{Q}_k = \begin{bmatrix} q_x \Sigma & \mathbf{0}_2 \\ \mathbf{0}_2 & q_y \Sigma \end{bmatrix}, \quad (20)$$

where $\mathbf{0}_2$ is zero matrix of indicated dimension, $\Sigma = \begin{bmatrix} \frac{dt^3}{3} & \frac{dt^2}{2} \\ \frac{dt^2}{2} & dt \end{bmatrix}$, $dt = 1$ $[s]$ is a sampling period, and $q_x = q_y = 0.05$.

- Known turn rate (TR) model with matrices

$$\mathbf{F}_k = \begin{bmatrix} 1 & \frac{\sin \omega dt}{\omega} & 0 & -\frac{1 - \cos \omega dt}{\omega} \\ 0 & \cos \omega dt & 0 & \sin \omega dt \\ 0 & \frac{1 - \cos \omega dt}{\omega} & 1 & -\frac{\sin \omega dt}{\omega} \\ 0 & \sin \omega dt & 0 & \cos \omega dt \end{bmatrix}, \quad (21)$$

$$\mathbf{Q}_k = \begin{bmatrix} q_x \Sigma & \mathbf{0}_2 \\ \mathbf{0}_2 & q_y \Sigma \end{bmatrix}, \quad (22)$$

with the turn rate $\omega = 20^\circ$.

- Known Known TR model with $\omega = -20^\circ$.

At any given time, targets have a finite probability of switching from one transition model to another according to transition probability matrix given by

$$\mathbf{T} = \begin{bmatrix} 0.7 & 0.15 & 0.15 \\ 0.4 & 0.6 & 0 \\ 0.6 & 0.4 & 0 \end{bmatrix}. \quad (23)$$

The target position is observed by the radar providing measurement of the range in $[m]$ and bearing in $[rad]$, which are related to the state using (2), where

$$\mathbf{h}_k(\mathbf{x}_k) = \begin{bmatrix} \sqrt{(\mathbf{x}_{1,k} - r_N)^2 + (\mathbf{x}_{3,k} - r_E)^2} \\ \arctan \frac{\mathbf{x}_{3,k} - r_E}{\mathbf{x}_{1,k} - r_N} \end{bmatrix}, \quad (24)$$

and $[r_N, r_E]^T = [0, 0]^T$ is the known radar position. The measurement is affected by the measurement noise \mathbf{v}_k with the covariance matrix

$$\mathbf{R} = \begin{bmatrix} 4 & 0 \\ 0 & 0.5(\pi/180)^2 \end{bmatrix}. \quad (25)$$

Detailed settings for the complete MTT system can be found linked github repository in the form of a Jupyter notebook.

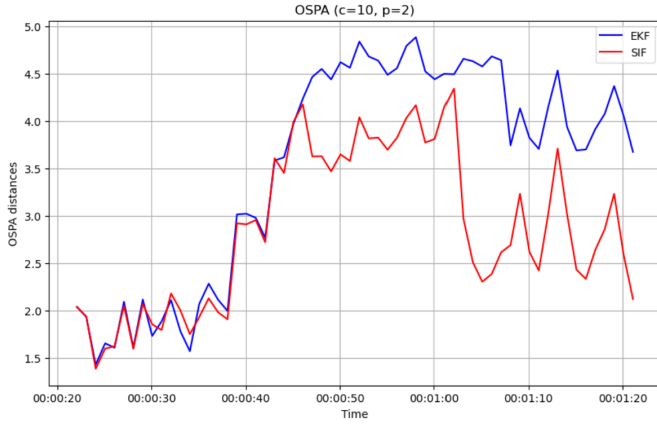


Fig. 2. OSPA metrics results for Class-B example.

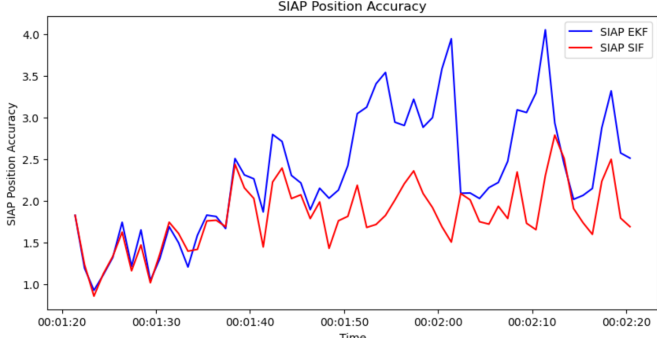


Fig. 3. SIAP position accuracy results for Class-B example.

B. Results

The SIF and EKF perform extremely similarly initially, before both filters spike in OSPA. The difference in overall shape of Fig. 2 and Fig. 3 highlight a key difference in OSPA and positional error as metrics. From time $k = 45$ onward, both the positional error and OSPA graphs show the EKF and SIF diverge from one another, but the OSPA graph shows a smaller relative difference between the two trackers. This is due to OSPA emphasizing cardinality errors more than locality errors, thus making the metric less sensitive to being skewed by lone outlier tracks which diverge.

The positional error graph in Fig. 3 shows that neither filter ever fully diverged or lost any of the targets. But the sum of

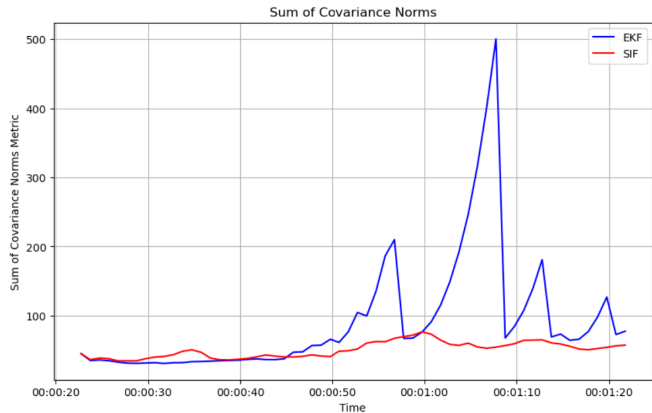


Fig. 4. Covariance norms metrics results for Class-B example.

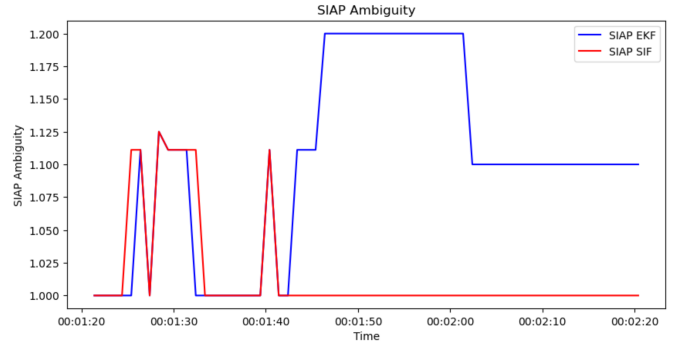


Fig. 5. SIAP Ambiguity Metric for Class-B example

covariance norms in Fig. 4 indicates that on several occasions the EKF saw massive spikes in uncertainty which are not present for the SIF. These spikes are due to association errors in which the EKF incorrectly distinguishes between two or more nearby targets.

In this example the SIF's advantages in covariance propagation enable it to distinguish between targets leading to a much more accurate set of tracks. These association errors can be directly observed clearly in the SIAP Ambiguity plot which shows the EKF these making incorrect associations.

VI. OPENSky ADS-B CLASS-A AIRSPACE DATASET

ADS-B is a standard aircraft surveillance technology in which aircraft determine their own position and heading via satellite navigation and broadcast it out at set intervals to air traffic control towers and other aircraft in the vicinity. The datasets gathered from aircraft ADS-B systems are freely available to the public and offer an easily accessible and realistic environment to test multi target tracking methods, e.g., via OpenSky Network [28]. However, the ADS-B data has some limitations for the purpose of Air Traffic Control such as (1) antenna positions, (2) bandwidth variations, (3) local policies, (4) data repository, and (5) interval rates. Hence, research challenges include coverage, GNSS validation, and decoding. These limitations along with the vulnerability of ADS-B to cyberattacks via spoofing false aircraft or jamming the broadcasts of true ones, necessitate MTT methods to ensure the integrity of the surveillance system.

A. Simulating Detections

In this example, the position and velocity data from aircraft in Great Britain is treated as the ground truth. Detections are simulated from two stationary points which broadly correspond to ground based radars located in Manchester airport and Heathrow airport in London. A third sensor is located on an airborne moving platform located with initial state at longitude and latitude $(52.25^\circ, -0.09^\circ)$, at an elevation $5 [km]$ above sea level, which is between the cities of Manchester and London. These coordinates were chosen specifically to deal with the finite range of the sensors [35]. The detections are converted from longitude and latitude, into bearing range, and angle of elevation format to simulate radar detections in three dimensions. A total of 84 aircraft are detected by the simulated

sensors and are tracked for as long as they remain in range of the sensors.

B. Tracker Parameters

In this scenario we expand the simulation from two dimensions via bearing and range, to three by considering the azimuth, elevation, and range model to expand the scenario to three dimensions. We also estimates a significantly higher number of aircraft. As such the transition models for estimating the velocity of aircraft changes and we consider the constant velocity model in three dimensions, with corresponding covariance matrix:

$$\mathbf{F}_k = \begin{bmatrix} 1 & dt & 0 & 0 & 0 & 0 \\ 0 & 1 & 0 & 0 & 0 & 0 \\ 0 & 0 & 1 & dt & 0 & 0 \\ 0 & 0 & 0 & 1 & 0 & 0 \\ 0 & 0 & 0 & 0 & 1 & dt \\ 0 & 0 & 0 & 0 & 0 & 1 \end{bmatrix},$$

$$\mathbf{Q}_k = \begin{bmatrix} q_x \Sigma & \mathbf{0}_2 & \mathbf{0}_2 \\ \mathbf{0}_2 & q_y \Sigma & \mathbf{0}_2 \\ \mathbf{0}_2 & \mathbf{0}_2 & q_z \Sigma \end{bmatrix},$$

with $q_x = 10$, $q_y = 10$, and $q_z = 5$. The aircraft are tracked by three radars providing measurement of the bearing, azimuth, and range

$$\mathbf{h}_k(\mathbf{x}_k) = \begin{bmatrix} \arcsin\left(\frac{\mathbf{x}_3}{\sqrt{(\mathbf{x}_{1,k}-r_N)^2 + (\mathbf{x}_{3,k}-r_E)^2 + (\mathbf{x}_{5,k}-r_D)^2}}\right) \\ \arctan\frac{\mathbf{x}_{3,k}-r_E}{\mathbf{x}_{1,k}-r_N} \\ \sqrt{(\mathbf{x}_{1,k}-r_N)^2 + (\mathbf{x}_{3,k}-r_E)^2 + (\mathbf{x}_{5,k}-r_D)^2} \end{bmatrix}, \quad (26)$$

with the zero-mean additive noise with the covariance matrix

$$\mathbf{R}_k = \begin{bmatrix} \sigma_\theta^2 & 0 & 0 \\ 0 & \sigma_\phi^2 & 0 \\ 0 & 0 & \sigma_r^2 \end{bmatrix} = \begin{bmatrix} (0.75\pi/180)^2 & 0 & 0 \\ 0 & (2\pi/180)^2 & 0 \\ 0 & 0 & 100^2 \end{bmatrix}$$

The radar position $[r_N, r_E, r_D]^T$ in three dimensional space which is assumed known for all three radars. This includes the radar on the moving platform. The maximum range of 111 [km] and the covariance parameters chosen here were picked to resemble the Airport Surveillance Radar 11 (ASR-11) [35].

C. Results

For the Class-A airspace example, the SIF demonstrated a marginal improvement over the EKF. At first glance a reasonable sounding explanation is that targets in this scenario do not perform maneuvers very often, as aircraft tend to ascend to cruising altitude where they travel at constant speed and heading. However, if model mismatch due to maneuvering targets were the dominant factor in the spiking error, then Fig. 4 would show corresponding spikes in covariance in the SIF curve which are not present in the Class-B Airspace example. This indicates that the similar performance of the two algorithms is instead explained by the fact that targets in Class-A airspace are so much farther apart, meaning that

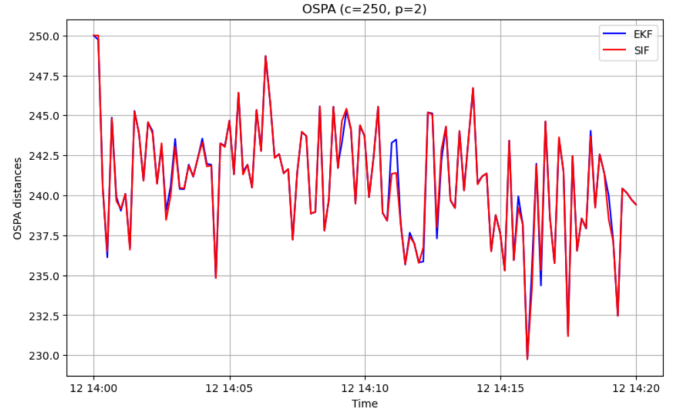


Fig. 6. OSPA metrics results for ADS-B Dataset

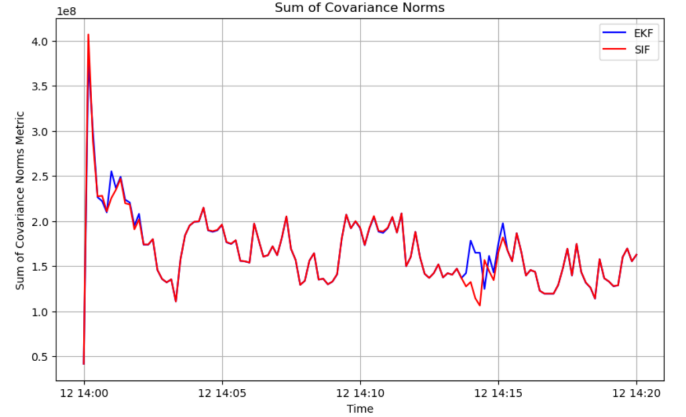


Fig. 7. Covariance norms metrics result for the ADS-B Dataset

target ambiguity is less of a concern. This can most evident in Fig. 8 which shows that none of the filters falsely associate detections. In this scenario the linearization of the EKF offers a sufficient approximation of the state uncertainty such that the benefits of the SIF do not prove decisive.

VII. CONCLUSIONS

In both examples the third order SIF demonstrated a notable albeit subtle performance uplift over the Extended Kalman Filter. While the differences were much smaller in the Class-A scenario, the SIF demonstrated a marginal improvement in covariance propagation which in turn led to a more consistent tracker. Where maximum performance is desired, the SIF

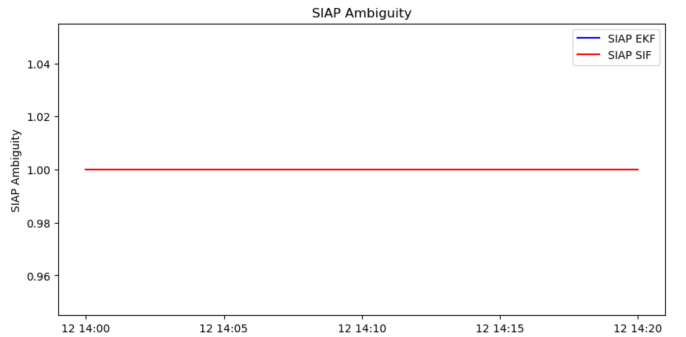


Fig. 8. SIAP Ambiguity Metric for Class-A example

offers a significant advantage in scenarios where the increased computational complexity of the SIF compared to the EKF is not a constraint. The SIF demonstrates particular promise in high density spaces with a large amounts of targets per zone where sensors may have trouble associating tracks to targets. This implies that the SIF may have a significant advantage in tracking targets in the presence of clutter, though this scenario was not tested in this paper and will be saved for follow up studies.

REFERENCES

- [1] Anderson, B.D.O., Moore, J.B.: Optimal Filtering. Prentice Hall, New Jersey (1979)
- [2] Arasaratnam, I., Haykin, S.: Cubature Kalman filters. *IEEE Trans. on Automatic Control* **54**(6) (2009) 1254–1269
- [3] Bar-Shalom, Y., Willett, P.K., Tian, X.: Tracking and Data Fusion: A Handbook of Algorithms. YBS Publishing, Storrs, CT (2011)
- [4] Barr, J., Harald, O., Hiscocks, S., Perree, N., Pritchett, H., Vidal, S., Wright, J., Carniglia, P., Hunter, E., Kirkland, D., Raval, D., Zheng, S., Young, A., Balaji, B., Maskell, S., Hernandez, M., Vladimirov, L.: Stone Soup open source framework for tracking and state estimation: enhancements and applications. Volume 12122., *SPIE* (2022) 1212205–1212205–17
- [5] Blackman, S.S., Popoli, R.F.: Design and Analysis of Modern Tracking Systems. Artech House (1999)
- [6] Blasch, E., Niu, R., O'Rourke, S.: Target tracking analysis for Stone Soup. In: *Int'l Conf. on Information Fusion*. (2020)
- [7] Chong, Z.Y., Pritchett, H., Li, Q., Gan, R., Kindap, Y., Godsill, S.: Implementation of non-gaussian motion models within Stone Soup. In: *2024 27th International Conference on Information Fusion (FUSION)*. (2024) 1–8
- [8] Duník, J., Matoušek, J., Straka, O., Blasch, E., Hiles, J., Niu, R.: Stochastic integration based estimator: Robust design and Stone Soup implementation. In: *Proc. 2024 27th International Conference on Information Fusion (FUSION)*. (2024)
- [9] Duník, J., Soták, M., Veselý, M., Straka, O., Hawkinson, W.J.: Design of Rao-Blackwellised point-mass filter with application in terrain aided navigation. *IEEE Transactions on Aerospace and Electronic Systems* **55**(1) (2019) 251–272
- [10] Duník, J., Straka, O., Šimandl, M.: Stochastic integration filter. *IEEE Transactions on Automatic Control* **58**(6) (2013) 1561–1566
- [11] Duník, J., Straka, O., Šimandl, M., Blasch, E.: Random-point-based filters: Analysis and comparison in target tracking. *IEEE Transactions on Aerospace and Electronic Systems* **51**(2) (2015) 1403–1421
- [12] Duník, J., Šimandl, M., Straka, O.: Unscented Kalman filter: Aspects and adaptive setting of scaling parameter. *IEEE Transactions on Automatic Control* **57**(9) (2012) 2411–2416
- [13] Evensen, G.: Data assimilation: The ensemble Kalman filter. Springer Verlag (2009)
- [14] Hiles, J., O'Rourke, S.M., Niu, R., Blasch, E.P.: Implementation of ensemble Kalman filters in stone-soup. In: *2021 IEEE 24th International Conference on Information Fusion (FUSION)*. (2021) 1–8
- [15] Julier, S.J., Uhlmann, J.K.: Unscented filtering and nonlinear estimation. *IEEE Proceedings* **92**(3) (2004) 401–421
- [16] Julier, S.J., Uhlmann, J.K., Durrant-Whyte, H.F.: A new method for the nonlinear transformation of means and covariances in filters and estimators. *IEEE Transactions on Automatic Control* **45**(3) (2000) 477–482
- [17] Mahler, R.: Statistical Multisource-Multitarget Information Fusion. Artech House (2007)
- [18] Mahler, R.: Advances in Statistical Multisource-Multitarget Information Fusion. Artech House (2014)
- [19] Meyer, F., Kropfreiter, T., Williams, J.L., Lau, R., Hlawatsch, F., Braca, P., Win, M.Z.: Message passing algorithms for scalable multitarget tracking. *Proceedings of the IEEE* **106**(2) (February 2018) 221–259
- [20] Nørgaard, M., Poulsen, N.K., Ravn, O.: Advances in derivative-free state estimation for nonlinear systems. Technical report, Technical University of Denmark. Department of Mathematical Modelling. Department of Automation (2000) IMM-REP-1998-15.
- [21] Nørgaard, M., Poulsen, N.K., Ravn, O.: New developments in state estimation for nonlinear systems. *Automatica* **36**(11) (2000) 1627–1638
- [22] OSTEWG: Welcome to Stone Soup's documentation! <https://stonesoup.readthedocs.io/en/v1.5/> (2025) Accessed: February 2025.
- [23] Rahmathullah, A.S., García-Fernández, A.F., Svensson, L.: Generalized optimal sub-pattern assignment metric. *arXiv preprint arXiv:1601.05585* (2016)
- [24] Randall, T.J.: Matrix computations, by gene h. golub and charles f. van loan. pp 476. 1983. isbn 0-8018-3010-9 (johns hopkins university press). *Mathematical gazette* **69**(448) (1985) 152–152
- [25] Ristic, B., Arulampalam, S., Gordon, N.: Beyond the Kalman Filter: Particle Filters for Tracking Applications. Artech House (2004)
- [26] RTCA: Minimum operational performance standards for global positioning system / wide area augmentation system airborne equipment. Standard, Radio Technical Commission for Aeronautics (RTCA) (December 2006)
- [27] Särkkä, S.: Bayesian Filtering and Smoothing. Cambridge University Press (2013)
- [28] Schäfer, M., Strohmeier, M., Lenders, V., Martinovic, I., Wilhelm, M.: Bringing up OpenSky: A large-scale ADS-B sensor network for research. In: *Proceedings of the 13th International Symposium on Information Processing in Sensor Networks*, Piscataway, NJ, USA, IEEE Press (2014) 83–94
- [29] Simon, D.: Optimal State Estimation: Kalman, H Infinity, and Nonlinear Approaches. Wiley-Interscience (2006)
- [30] Song, P.X.K.: Monte Carlo Kalman filter and smoothing for multivariate discrete state space models. *Canadian Journal of Statistics* **28**(3) (2000) 641–652
- [31] Thomas, P.A., Barr, J., Balaji, B., White, K.: An open source framework for tracking and state estimation ('stone soup'). In: *SPIE Proceedings*. Volume 10200., *SPIE* (2017) 1020008–1020008–10
- [32] Vo, B.N., Vo, B.T., Phung, D.: Labeled random finite sets and the Bayes multi-target tracking filter. *IEEE Trans. Signal Process.* **62**(24) (Dec. 2014) 6554–6567
- [33] Votruba, P., Nisley, R., Rothrock, R., Zombro, B.: Single integrated air picture (SIAP) metrics implementation. Technical report (October 2001) Technical Report.
- [34] Šimandl, M., Duník, J.: Derivative-free estimation methods: New results and performance analysis. *Automatica* **45**(7) (2009) 1749–1757
- [35] Weber, M.E.: Faa surveillance radar data. Technical report (2000) Technical Report, Massachusetts Institute of Technology.
- [36] Wright, J.S., Sun, M., Davies, M.E., Proudler, I.K., Hopgood, J.R.: Implementation of AKKF-based multi-sensor fusion methods in Stone Soup. In: *2024 27th International Conference on Information Fusion (FUSION)*. (2024) 1–7
- [37] Zhou, D., Guo, L.: Stochastic integration hinfinitly filter for rapid transfer alignment of ins. *Sensors* **17**(11) (2017)